

# Superflares on Solar-Type Stars Observed with Kepler

## II. Photometric Variability of Superflare-Generating Stars : A Signature of Stellar Rotation and Starspots

Yuta Notsu<sup>1</sup>, Takuya Shibayama<sup>1</sup>, Hiroyuki Maehara<sup>2,3</sup>, Shota Notsu<sup>1</sup>, Takashi Nagao<sup>1</sup>,  
Satoshi Honda<sup>2,4</sup>, Takako T. Ishii<sup>2</sup>, Daisaku Nogami<sup>2</sup>, and Kazunari Shibata<sup>2</sup>

<sup>1</sup>Department of Astronomy, Faculty of Science, Kyoto University,  
Kitashirakawa-Oiwake-cho, Sakyo-ku, Kyoto, 606-8502, Japan

<sup>2</sup>Kwasan and Hida Observatories, Kyoto University, Kitakazan-ohmine-cho, Yamashina-ku,  
Kyoto, 607-8471, Japan

<sup>3</sup>Kiso Observatory, Institute of Astronomy, School of Science, The University of Tokyo,  
10762-30, Mitake, Kiso-machi, Kiso-gun, Nagano 397-0101, Japan

<sup>4</sup>Center for Astronomy, University of Hyogo, 407-2, Nishigaichi, Sayo-cho, Sayo, Hyogo,  
679-5313, Japan

ynotsu@kwasan.kyoto-u.ac.jp

Received \_\_\_\_\_; accepted \_\_\_\_\_

## ABSTRACT

We performed simple spot-model calculations for quasi-periodic brightness variations of solar-type stars showing superflares, by using Kepler photometric data. Most of superflare stars show quasi-periodic brightness modulations with the typical period of one to a few tens of days. Our results indicate that these brightness variations of superflare stars can be explained by the rotation of the star with fairly large starspots. Using the result of the period analysis, we investigated the relation between the energy and frequency of superflares and the rotation period. Stars with relatively slower rotation rates can still produce flares that are as energetic as those of more rapidly rotating stars, although the average flare frequency is lower for more slowly rotating stars. We found that the energy of superflares are related to the total coverage of starspots. The correlation between the spot coverage and the flare energy in superflares is similar to that in solar flares. These results suggest that the energy of superflares can be explained by the magnetic energy stored around starspots.

*Subject headings:* stars: activity — stars: flare — stars: rotation — stars: solar-type  
— stars: spots

## 1. Introduction

Solar flares are the most energetic explosions on the surface of the Sun, and are thought to occur by release of magnetic energy (e.g., Shibata & Magara 2011). Flares are also known to occur on various types of stars including solar-type stars (Schaefer 1989; Gershberg 2005). Among them, young stars or close binary stars sometimes produce "superflares", flares whose total energy is  $10 \sim 10^6$  times more energetic ( $\sim 10^{33-38}$  erg) than the largest flares on the Sun ( $\sim 10^{32}$ erg) (Schaefer et al. 2000). Such stars generally rotate fast ( $v_{\text{rot}} \sim$  a few  $10 \text{ km s}^{-1}$ ), and the magnetic fields of a few kG are considered to be distributed in large regions on the stellar surface (Gershberg 2005; Shibata & Yokoyama 1999, 2002). In contrast, the Sun slowly rotates ( $v_{\text{rot}} \sim 2 \text{ km s}^{-1}$ ), and the magnetic fields are weak. Here we define "Sun-like" stars as solar-type stars slowly rotating and whose surface temperature is  $5,600\text{K} \sim 6,000\text{K}$ . It has been thought that superflares cannot occur on Sun-like stars.

Schaefer et al. (2000), however, found 9 candidates of superflares on slowly rotating stars like the Sun. This is extremely important in many fields including magnetic activity research in solar/stellar physics as well as the planetary habitability in astrobiology (e.g., Segura et al. 2010). The frequency, detailed properties, and mechanism of the superflares are, however, still not clear because of lack of observations. Therefore, it is necessary to investigate in detail how often superflares occur on solar-type stars, properties of superflares, and stellar conditions which lead to superflares.

We have already analyzed the data by the Kepler spacecraft (Koch et al. 2010), and discovered 365 superflare events on 148 solar-type stars that have surface temperature of  $5,100\text{K} \leq T_{\text{eff}} < 6,000\text{K}$ , and surface gravity of  $\log g \geq 4.0$  (Maehara et al. 2012). The Kepler spacecraft is very useful to detect faint brightness increases in the stellar brightness due to stellar flares because Kepler realized high photometric precision and continuous

time-series data of a lot of stars over a long period (Walkowicz et al. 2011; Balona 2012). We found that superflares whose energy is  $10^2 - 10^3$  times larger than that of the most energetic flare on the Sun, can occur on solar-type stars once in a few thousands of years. Many of solar-type stars having superflares show quasi-periodic brightness variations with the typical period from one day to a few tens of days. Such variations can be explained by the rotation of the star (e.g., Basri et al. 2011; Debosscher et al. 2011; Harrison et al. 2012).

In this paper, we investigate the brightness variations of superflare-generating stars by considering the signature of stellar rotation and starspots. First we show that the brightness variation of some typical superflare-generating stars are explained by the rotation of a star with starspots, by simple model analyses. Our main purpose of the model analysis is to demonstrate that the brightness variations include the information of the overall areal coverage by starspots and the rotation periods of superflare stars. Second, using the result of the period analysis, we consider relations between the rotation period and properties of superflares such as flare energy and flare frequency. Third, we discuss relations between the starspot coverage and the energy of superflares by assuming that the brightness variations are due to the rotation. For the Sun, it has been known that there is a positive correlation between the sunspot coverage and the energy of the largest flare observed, and that the energy of the largest flare depends on the magnetic energy stored around the sunspots (e.g., Sammis et al. 2000). We then investigate whether this correlation can be applied to superflare-generating stars, and discuss the relations between the magnetic energy of starspots and the superflare energy.

The details of Kepler data we use in this paper are explained in Section 2. We show in Section 3 the results of the spot modeling for some typical superflare-generating stars. We consider the relation between the rotation period and properties of superflares,

on the basis of the results of the period analysis in Section 4. We discuss the relation between the starspot coverage and the energy of superflares by assuming that the brightness variations of superflare-generating stars are due to the rotation in Section 5.

## 2. Observational Data and Period Analysis

We searched for flares on solar-type stars using the Kepler data which was taken during the period from April 2009 to September 2010 (quarter 0~6). These data were retrieved from the Multimission Archive at Space Telescope Science Institute (MAST)<sup>1</sup>. We used the effective temperature ( $T_{\text{eff}}$ ) and the surface gravity ( $\log g$ ) in the Kepler Input Catalog (Brown et al. 2011) to select solar-type stars. The selection criteria are as follows;  $5,100 \leq T_{\text{eff}} < 6,000$ , and  $\log g \geq 4.0$ . The total number of solar-type stars is about 90,000. The length of the observation period during each quarter and the number of solar-type stars are summarized in Table 1.

We analyzed the long-cadence (time resolution of about 30 min) flux detrended by PDC-MAP pipeline (Stumpe et al. 2012) for detection of superflares. Details on the detection method are described in Maehara et al. (2012) and Shibayama et al. (2013). The version of the data we use in this paper are shown in Table 1.

Figure 1 shows the typical light curves of solar-type stars having superflares (KIC6034120 & KIC6691930, Quarter 2; KIC10528093, Quarter 0-2). KIC6034120 shows a lightcurve of a simple sine-like profile which can be well reproduced with one large starspot. The lightcurve of KIC6691930 requires two starspots to explain the shoulder of the rising

---

<sup>1</sup><http://archive.stsci.edu/kepler/>

part. KIC10528093 also needs two starspots, and its long-term amplitude variation cannot be explained by the solid rotation model. These parts of the data are selected to make these features clearly demonstrated. Light curves of all solar-type stars having superflares reported in Shibayama et al. (2013) are shown in Online-only Figures. The period of the brightness variation was estimated by the discrete Fourier transform (DFT) method. We carried out the following 5 procedures: (1) We measured the standard deviations ( $\sigma$ ) of the data in each quarter, and deleted all the data of a quarter whose  $\sigma$  value is over three times larger than the mean value. (2) The linear trend was removed in the brightness during each quarter. (3) The gaps in the mean brightness between each quarter were adjusted. (4) We took the power spectra of the period from 0.1 day to 45 day, since the reduction pipeline seems to generate spurious peaks at timescales longer than 45 days, a half of typical lengths of each quarter<sup>2</sup>. (5) We chose the peak in the power spectrum whose amplitude has the highest ratio to the red noise spectrum (e.g., Press 1978; Vaughan 2005) as the period of the brightness variation of the star, since in some cases simply taking the highest peak can lead to choose spurious peaks at long timescales. Figure 2 is the results of the period analysis for the brightness variation shown in Figure 1. Such stars show quasi-periodic brightness variations with the typical period from one day to a few tens of days.

---

<sup>2</sup>For the detrend method by the Kepler pipeline, see <http://keplergo.arc.nasa.gov/PyKEprimerCBVs.shtml>

### 3. Model Calculation of Brightness Variation of Rotating Stars with Large Starspots

We performed simple calculations to show that brightness variations of superflare-generating stars can be explained by their rotation and the presence of large starspots. There are many former researches which calculate the brightness variation by assuming the existence of dark spots on the surface of the star (e.g., Budding 1977; Dorren 1987; Eker 1994). Spot modeling has much uncertainty and it is almost impossible to get unique solutions from the spot modeling (e.g., Eker (1996); Kovari & Bartus (1997); Walkowicz et al. (2013)). There are many parameters such as inclination angle and spot latitude which affect the shape of the lightcurve. In addition, the Kepler spacecraft provides only single color photometry data, and this also generates degeneracy between the spot size and the spot contrast. Our main purpose is to demonstrate that the brightness variations include the information of the overall areal coverage by starspots and the rotation periods of superflare stars.

Our method of the spot modeling is as follows. We regard the total luminosity of the photosphere, and the starspot area as a good representation of the flux ( $F$ ) in our modeling. The shape of the model star is assumed to be a sphere, and some circular spots are placed on the photosphere. It should be noted that we do not exclude the possibility that starspots of superflare stars are collections of smaller spots. The surface of the star is divided into 180 pieces ( $j$ ) in the latitudinal angle and into 360 pieces ( $k$ ) in the longitudinal angle. The contributions to the total brightness are summed up from each piece ( $f_{j,k}$ ) as follows;

$$F \propto \sum_{j,k} f_{j,k} , \quad (1)$$

and

$$f_{j,k} = \begin{cases} f_{j,k}^{\text{spot}} \text{ (in the spot area)} \\ f_{j,k}^{\text{phot}} \text{ (out of the spot area)} . \end{cases} \quad (2)$$

The temperature of the photosphere ( $T_{\text{phot}}$ ) and that of the spot area ( $T_{\text{spot}}$ ) are here considered to be the same over the solar photosphere (6,000K) and the sunspot area (4,000K, cf. Berdyugina 2005), respectively. The luminosity of each piece which is in the starspot area is estimated by

$$f_{j,k}^{\text{spot}} = \begin{cases} \sigma_{\text{SB}} T_{\text{spot}}^4 S_{\text{pix}} \mathbf{n}_{j,k} \cdot \mathbf{a}_{j,k} & (\mathbf{n}_{j,k} \cdot \mathbf{a}_{j,k} \geq 0) \\ 0 & (\mathbf{n}_{j,k} \cdot \mathbf{a}_{j,k} < 0) \end{cases}, \quad (3)$$

where  $S_{\text{pix}}$  and  $\mathbf{n}_{j,k}$  is a size and a normal vector of each pixel, respectively, and  $\mathbf{a}_{j,k}$  is a unit vector which is antiparallel to the line of sight.  $\sigma_{\text{SB}}$  is the Stefan-Boltzmann constant.

The luminosity of each piece which is out of the starspot area is estimated by

$$f_{j,k}^{\text{phot}} = \begin{cases} \sigma_{\text{SB}} T_{\text{phot}}^4 S_{\text{pix}} \mathbf{n}_{j,k} \cdot \mathbf{a}_{j,k} & (\mathbf{n}_{j,k} \cdot \mathbf{a}_{j,k} \geq 0) \\ 0 & (\mathbf{n}_{j,k} \cdot \mathbf{a}_{j,k} < 0) \end{cases}. \quad (4)$$

We also take into the effect of limb darkening. Applying the equation (1) in Sing (2010), this effect is calculated by

$$\frac{f_{j,k}(\mu)}{f_{j,k}^{\text{NLD}}} = 1 - u(1 - \cos \mu), \quad (5)$$

where  $f_{j,k}^{\text{NLD}}$  is the luminosity of each piece without the limb-darkening effect,  $f_{j,k}(\mu)$  is that with the limb-darkening effect,  $\mu = \cos \Theta$  and  $\Theta$  is the viewing angle. We here assume  $u = 0.6$  on the basis of Figure 3 in Claret (2004). Because of the rotation, the visibility of the starspots changes, and the brightness then varies. We calculate the brightness by changing the angle of rotation by 1 degree. Model light curves are drawn with arbitrarily changing the spot position, spot radius, and inclination angle  $i$ , which is the angle between the line of sight and the rotation axis of the star. We selected cases which show rough agreement between the model and the observation by eye.

Figures 3, 4, and 5 show results of the spot model calculation for the brightness variations of typical solar-type stars having superflares in Figure 1 (KIC6034120,



KIC6691930, and KIC10528093). The stellar parameters of these stars are shown in Table 2. The period of the brightness variations of these stars is about 5~15 days, and the amplitude is from 0.1% to a few %.

As shown in Figure 3, the simple sine-like light curve of KIC6034120 can be reproduced by the model with one spot. Figure 3 (a) shows the model light curve for KIC6034120. The best set of model parameters are listed in Table 3. Snapshots of the modeled star are displayed in Figure 3 (b) and (c), which shows the star has a large spot compared to the Sun. Figure 3 (d) shows the comparison of observed light curve and the model light curve.

The shape of the light curve of KIC6691930 has one peak and one shoulder as shown in Figure 1 (b). The features can be reproduced by the two spot model as shown in Figure 4. The longitude difference between two spots can be estimated by measuring the rotational phase of the shoulder in the light curve. Figure 4 (a) shows the model light curve for KIC6691930. The model parameters are listed in Table 3. Figure 4 (b), (c), and (d) are drawn for KIC6691930 in the same manner of Figure 3 (b), (c), and (d) for KIC6034120.

The shape of the light curve of KIC10528093 also has a shoulder as shown in Figure 1 (c). However, the long-term amplitude variation cannot be reproduced by a simple model with two spots in solid body rotation since the phase of the shoulder changes as time progresses.

These variations can be explained by the differential rotation (e.g., Frasca et al. 2011; Fröhlich et al. 2012). Here, we consider the two-spot model with the differential rotation. It should be noted that what this model shows is only that the differential rotation in this model is of approximately the correct amount. This is because a qualitatively

similar fit would be produced by any models, with almost any spot parameters, which get the amount of the differential rotation correct and the rough longitudinal separation correct. Parameters of the differential rotation (the dependence of the rotation speed on the latitude) we use here is based on the value for the Sun (Snodgrass & Ulrich 1990). The relation between the angular velocity of the rotation ( $\omega$ ) and the latitude ( $\varphi$ ) is represented by the equation (6).

$$\omega = A + B \sin^2 \varphi + C \sin^4 \varphi . \quad (6)$$

For the Sun, the values of  $A$ ,  $B$  and  $C$  are as follows;  $A = 14.71 \text{ deg day}^{-1}$ ,  $B = -2.39 \text{ deg day}^{-1}$ , and  $C = -1.78 \text{ deg day}^{-1}$  (Snodgrass & Ulrich 1990). We here ignore the “ $C \sin^4 \varphi$ ” term since this term is negligibly small in our model, and then we convert values  $A$  and  $B$  to ones which corresponds to the rotation period of KIC10528093. For KIC10528093, the value of  $A$  and  $B$  are as follows;  $A = 31.1 \text{ deg day}^{-1}$ , and  $B = -5.05 \text{ deg day}^{-1}$ . Figure 5 (a) shows the model light curve for KIC10528093. The model parameters are listed in Table 3. Snapshots of the modeled star are shown in Figure 5 (b), (c), (d), and (e). We compare the observed light curve with modeled light curve in Figure 5 (f). Figure 6 shows power spectra of the observed light curve and the model light curve in Figure 5 (f). We can see that the feature of the power spectrum, that is, the dominant and overtone peaks, and the slope to the higher frequencies, is also roughly reproduced with our spot model.

Consequently, most of the brightness variations with the period of a few days to a few tens of days and the amplitude of  $0.1 \sim 10\%$  are expected to be able to be explained by assuming that the star has fairly large starspots.

#### 4. Ensemble Properties of Superflares: Dependence of Flare Energy and Flare Frequency on Rotation Period

Applying the results shown in Section 3, we assume that many of the brightness variations of solar-type stars with superflares can be explained by their rotation and the presence of large starspots. Only three particular lightcurves were shown to be roughly reproduced by our uncomplicated model calculations in the above section. This does not prove that such spot models can be applied to the lightcurves of all the superflare stars.

Figure 7 shows the relations between the rotation period and the features of superflares. Although the similar relations have been already discussed in Maehara et al. (2012), we here add data of superflares we newly found in Shibayama et al. (2013) from Kepler quarter 3-6 data and improve the statistical precision by increasing the numbers of data. The rotation periods are determined by using the way described near the end of section 2, although this way includes some uncertainty (e.g., Walkowicz et al. 2013). Figure 7 (a) indicates that the most energetic flare observed in a given rotation period bin does not have a correlation with the period of stellar rotation. If the superflare energy can be explained by the magnetic energy stored near the starspots (we discuss this in Section 5), this result suggests that the maximum magnetic energy stored near the spot does not have a strong dependence on the rotation period. Figure 7 (b) shows that the average flare frequency in a given period bin tends to decrease as the period increases to periods longer than a few days. The value of the frequency is the average of all superflare stars in the same period bin. Some of superflare stars (e.g., examples in Figure 1) are then able to have higher frequencies of superflares. The frequency of superflares on rapidly rotating stars is higher than slowly rotating stars. It is known that the rotation period correlates with the chromospheric activity and the more rapidly rotating stars have higher magnetic activity (e.g., Noyes et al. 1984 ; Pallavicini et al. 1981). These imply that rapidly rotating stars

with high magnetic activity can generate more frequent superflares.

## 5. Discussion on starspot coverage and Energy of superflares

As described in Section 1, it has been said that the brightness variation of many solar-type stars observed by Kepler is due to the rotation of the star with starspots. This effect of rotation is also seen in the Sun. Figure 8 represents that there are also the same relations in the Sun; changes of the visible area of the sunspot causes the brightness variation. However, faculae also can affect the brightness variations of the Sun (e.g., Lanza et al. 2003). The brightness variations of superflare-generating stars are also probably somewhat affected by faculae, though Lockwood et al. (2007) indicates that the photometric behaviors of (young) active stars are dominated by starspots. In this paper, we do not include the faculae effects when analyzing the Kepler data, as described in Walkowicz et al. (2013).

Maehara et al. (2012) showed that superflare-generating stars have the brightness variation with the period of a few days to several tens of days, and that many of such variations are likely due to the rotation, though the possibility that the star is a binary is not completely excluded. It is well known that more than half of general solar-type stars are binary (e.g., Duquennoy & Mayor 1991). However photometric observations by Kepler mission cannot detect spectroscopic binaries. We cannot exclude the possibility that superflares are taking place on the spectroscopic binary companions. Because of this, the period data shown in Figure 7 are not necessarily due to rotation, and in particular the target with a 0.1-day periodicity is probably a binary. Spectroscopic observation is necessary, which will be our future project (e.g., Notsu et al. 2013a).

Here we assume the brightness variations are due to the rotation. Our model analyses for some typical brightness variations suggest us that, if we take into account the effects of some parameters, such as, the inclination angle, and the spot latitude, the brightness variations whose amplitude is about 0.1~10% can be well explained by the rotation of the star with fairly large starspots.

In the following, we discuss the relation between the starspot coverage and the energy of superflares. Flares are the release of the stellar magnetic energy (e.g., Shibata & Magara 2011). It is known that there are positive correlations between the sunspot coverage and the energy of the largest solar flares (Sammis et al. 2000). It is, therefore, important to consider whether the same correlations can be found and the observed maximum of superflare energy can be explained by the magnetic energy of large starspots which many of the superflare stars are expected to have. Although we have already simply discussed the relation between the amplitude of superflares and that of the brightness variations in Supplementary Information Section of Maehara et al. (2012), we here advance this former analysis and discuss whether the magnetic energy of starspots can well explain the energy of superflares by applying the results in this paper that starspot coverages can be roughly estimated from the brightness variation.

First, we discuss expected relations if the energy sources of superflares are the magnetic energy stored around the starspots ( $E_{\text{flare}} \leq E_{\text{mag}}$ ). The total energy released by the flare must be smaller than (or equal to) the magnetic energy stored around the starspots. The order of the stored magnetic energy ( $E_{\text{mag}}$ ) can be roughly estimated by

$$E_{\text{mag}} \approx \frac{B^2 l^3}{8\pi}, \quad (7)$$

where  $B$  and  $l$  correspond to the magnetic field strength and the size of the starspot region. It should be noted that we cannot exclude the possibility that starspots of superflare stars are collections of smaller spots.

We roughly assume that there is a linear correlation between the brightness variation and the spot coverage when we estimate the magnetic energy stored around the starspots from the amplitude of the brightness variation. The total amplitude of the brightness variation due to the rotation normalized by the average brightness ( $\Delta F_{\text{rot}}$ ) can be expressed by

$$\Delta F_{\text{rot}} \approx \left[ 1 - \left( \frac{T_{\text{spot}}}{T_{\text{phot}}} \right)^4 \right] \frac{A_{\text{spot}}}{A_{\text{phot}}} , \quad (8)$$

where  $A_{\text{spot}}$  is the total area of starspots, and  $A_{\text{phot}}$  is the total visible area of the stellar surface. Since the Kepler photometer covers a wide spectral range (4,000 ~ 8,500Å), observed brightness changes would be nearly approximated by the bolometric brightness change obtained by the equation (8).

If we assume that  $l^3 \approx A_{\text{spot}}^{3/2}$ , the equation (7) can be transformed to

$$E_{\text{mag}} \approx \frac{B^2}{8\pi} A_{\text{spot}}^{3/2} \approx \frac{B^2}{8\pi} \left( \frac{A_{\text{phot}} \Delta F_{\text{rot}}}{1 - (T_{\text{spot}}/T_{\text{phot}})^4} \right)^{3/2} \geq E_{\text{flare}} , \quad (9)$$

where  $E_{\text{flare}}$  is the total energy released by the flare. The amplitude of the flare normalized by the average brightness ( $\Delta F_{\text{flare}}$ ) can be estimated by

$$\Delta F_{\text{flare}} \approx \frac{E_{\text{flare}}}{L_{\text{star}} \tau} , \quad (10)$$

where  $L_{\text{star}}$  is the luminosity of the star, and  $\tau$  is the e-folding time of the flare. Then the relation between the flare amplitude and the brightness variation amplitude can be written as

$$\Delta F_{\text{flare}} \leq \frac{B^2}{8\pi} \frac{A_{\text{spot}}^{3/2}}{L_{\text{star}} \tau} \approx \frac{B^2}{8\pi} \frac{1}{L_{\text{star}} \tau} \left( \frac{A_{\text{phot}} \Delta F_{\text{rot}}}{1 - (T_{\text{spot}}/T_{\text{phot}})^4} \right)^{3/2} \propto A_{\text{spot}}^{3/2} \propto (\Delta F_{\text{rot}})^{3/2} . \quad (11)$$

This indicates that the upper limit of the flare amplitude is proportional to 1.5 power of the starspots area if we assume  $B = \text{constant}$ . We discuss in the following whether this assumption is right.

The discussion described around equations (7)~(11) does not take into account the effect of the inclination angle  $i$  and spot latitude. In stars with lower inclination angle and higher spot latitude, the amplitude of brightness variation is smaller. If we consider inclination effects and assume the spot is distributed around the equator, equation (11) can be replaced by equation (12).

$$\Delta F_{\text{flare}} \leq \frac{B^2 (A_{\text{spot}}/\sin i)^{3/2}}{8\pi L_{\text{star}}\tau} \approx \frac{B^2}{8\pi L_{\text{star}}\tau} \left( \frac{A_{\text{phot}}\Delta F_{\text{rot}}}{1 - (T_{\text{spot}}/T_{\text{phot}})^4} \frac{1}{\sin i} \right)^{3/2}. \quad (12)$$

If we adopt  $L_{\text{star}} = 10^{33} \text{erg s}^{-1}$ ,  $\tau = 10^4 \text{sec}$ ,  $T_{\text{spot}} = 4,000 \text{K}$  and  $T_{\text{phot}} = 6,000 \text{K}$  for superflares on solar-type stars, then the flare amplitude can be roughly estimated by

$$\Delta F_{\text{flare}} \propto 10 \left( \frac{B}{1000 \text{G}} \right)^2 \left( \Delta F_{\text{rot}} \frac{1}{\sin i} \right)^{3/2}. \quad (13)$$

Figure 9 is the scatter plot of the superflare amplitude as a function of the amplitude of the brightness variation. The data of superflares are taken from quarter 1-6 data and are reported in Shibayama et al. (2013). The lines in this figure represent the analytic relation between the flare amplitude and the amplitude of the brightness variation obtained from equation (13) for  $i=90$  degree and  $i=2$  degree (nearly pole-on) case each. Taking into account that magnetic energy density of solar-type stars is about 1,000 ~ 4,000G (Solanki 2003), we show two lines ( $B=1,000 \text{G}$  & 3,000G) each. These lines give an upper limit for the flare amplitude based on the above discussion. Many of the flares have smaller amplitudes than that expected by the equation (13). Moreover all flares have smaller flare amplitudes than that expected in the nearly pole-on case (dashed-line;  $i=2$  degree). This

supports that the energy released by these flares can be explained by the magnetic energy stored near the starspots.

For the solar flares, there is a similar relation as this (Sammis et al. 2000). Figure 10 shows the empirical relation between the spot group area and X-ray intensity of solar flares (Sammis et al. 2000), and the relation between the spot group area (estimated from the brightness variation amplitude) and the superflare energy. It should be noted that while there is a large range in observed flare energies for a given sunspot area, we here in particular refer to the upper envelope of the observations shown in Figure 10, where the largest flare energies are associated with larger spots. The bolometric luminosity and the total bolometric energy of superflares were estimated from the stellar radius, the effective temperature in the Kepler Input Catalog (Brown et al. 2011), observed amplitude and duration of flares by assuming that the spectrum of white light flares can be described by the blackbody radiation with the effective temperature of  $\sim 10,000\text{K}$  (Kretzschmar 2011). Using concrete numerical values, equation (9) is transformed as

$$\begin{aligned}
 E_{\text{mag}} &\approx \frac{B^2}{8\pi} A_{\text{spot}}^{3/2} \\
 &\approx 10^{33}[\text{erg}] \left(\frac{B}{10^3\text{G}}\right)^2 \left(\frac{A_{\text{spot}}}{3 \times 10^{19}\text{cm}^2}\right)^{3/2} \\
 &\approx 10^{33}[\text{erg}] \left(\frac{B}{10^3\text{G}}\right)^2 \left(\frac{A_{\text{spot}}/(2\pi R_{\odot}^2)}{0.001}\right)^{3/2} \\
 &\geq E_{\text{flare}} ,
 \end{aligned} \tag{14}$$

where  $R_{\odot}$  is the radius of the Sun. The relation expressed by equation (14) can be seen in Figure 10. All of the solar flare data, and over a half of the superflare data are located below the same line of  $B=1,000\text{G}$ , and  $i=90\text{deg}$ .

Some data points of superflares are located above the line of equation (14). This is explained by the two reasons discussed in the following. First, the inclination and latitude



of the spots govern their projected area, and the size of the spot cannot be uniquely determined because of these effects and the fixed contrast with the photosphere. Lower inclinations cause a smaller projected spot area and/or the spot to be visible through most of the rotation period, and therefore lower brightness variations result in these cases.

Second, magnetic flux density ( $B$ ) is not necessarily constant. It is a function of the spot size. Solanki (2003) shows that the umbral continuum intensity of sunspots becomes weak as sunspots become large and that the intensity also becomes weak as the magnetic flux density gets strong. This fact means that as the spot becomes larger, the magnetic flux density becomes strong and the magnetic energy stored near the spot increases. As a result, the released flare energy tends to be bigger than that in the case of  $B=constant$ , and the straight lines in Figure 10 become steeper.

In this paper, we showed that many of superflare-generating stars probably have large starspots, and the energy of superflares can be explained by the magnetic energy stored around such starspots. We also confirmed in Section 4 the stellar activity depends on the rotation period. Stars with relatively slower rotation rates can still produce flares that are as energetic as those of more rapidly rotating stars, although the average flare frequency is lower for more slowly rotating stars. There are, however, many things to be left for consideration in the next step. For example, it is extremely important to know lifetime of starspot regions or how activity level changes because it is related to knowing how the starspot evolves by the dynamo mechanism. Shibata et al. (2013) indicated that the magnetic energy to generate superflares can be produced by the effects of differential rotation. We need to investigate in detail the effects of differential rotation on the brightness variation.

In addition, if superflares occur on the starspot area of a single star and the bright-

ness variation is caused by the rotation, the timings when superflares occur are likely to have a phase dependence, since superflares which we can observe need to occur when the starspots are on the visible side of the star. This phase dependence, however, is expected not to be necessarily true. For some pairs of spot distribution on the stellar surface and stellar inclination angle, some part of the area covered by the starspots is always on the visible side of the star. In these cases, it is probable that superflare occurs in any phase of the differential rotation. We need to study these effects in detail in the next step (cf. Roettenbacher et al. (2013) discuss these effects for one K-type star.).

## 6. Summary

In this paper, we investigated the brightness variations of superflare-generating stars in Kepler quarter 0-6 data by considering the signature of stellar rotation and the starspots. First, we performed simple spot model analyses for typical superflare-generating stars. Many of the brightness variations with the period of one day to a few tens of days and the amplitude of  $0.1 \sim 10\%$  can be explained by the rotation of the star with fairly large starspots, taking into account the effects of the inclination angle and the spot latitude. Next, using the result of the period analysis, we investigated the relations between the energy and frequency of superflares and the rotation period by assuming that the period of the brightness variation corresponds to the rotation period. Stars with relatively slower rotation rates can still produce flares that are as energetic as those of more rapidly rotating stars, although the average flare frequency is lower for more slowly rotating stars. Last, we discussed the relations between the starspot coverage and the energy of flares. If we assume that the brightness variations are due to the rotation, the energy of superflares can be explained by the magnetic energy stored near the large starspots.

We are grateful to Prof. Kazuhiro Sekiguchi (NAOJ) for useful suggestions. We also thank the anonymous referee for helpful comments. Kepler was selected as the tenth Discovery mission. Funding for this mission is provided by the NASA Science Mission Directorate. The data presented in this paper were obtained from the Multimission Archive at STScI. This work was supported by the Grant-in-Aid from the Ministry of Education, Culture, Sports, Science and Technology of Japan (No. 25287039).

## REFERENCES

- Balona, L. A., 2012 MNRAS, 423, 3420
- Basri, G., Walkowicz, L. M., Batalha, N., et al. 2011, AJ, 141, 20
- Benz, A., 2010 ARA&A, 48, 241
- Berdyugina, S. V., 2005, Living rev. Solar Phys., 2, 8
- Brown, T. M., Latham, D. W., Everett, M. E., & Esquerdo, G. A. 2011, ApJ, 142, 112
- Budding, E. 1977, Ap&SS, 48, 207
- Christiansen, J. & Barclay, T. 2012, Kepler Data Release 14 Notes, KSCI-19054-001,
- Christiansen, J. & Barclay, T. 2012, Kepler Data Release 16 Notes, KSCI-19056-001,
- Claret, A. 2004, A&A, 428, 1001
- Debosscher, J., Blomme, J., Aerts, C., & De Ridder, J. 2011, A&A, 529, A89
- Dorren, J. D. 1987, ApJ, 320, 756
- Duquennoy, A., & Mayor, M. 1991, A&A, 248, 485
- Eker, Z. 1994, ApJ, 420, 373
- Eker, Z. 1996, ApJ, 473, 388
- Frasca, A., Fröhlich, H.-E., Bonanno, A., et al. 2011, A&A, 532, A81
- Fröhlich, H.-E., Frasca, A., Catanzaro, G. et al. 2012, A&A, 543, A146
- Gershberg, R. E. 2005, Solar-Type Activity in Main-Sequence Stars (Berlin: Springer)
- Harrison, T. E., Coughlin, J. L., Ule, N. M., & Lopez-Morales, M. 2012, AJ, 143, 4

- Ishii, T. T. 2012, private communication
- Koch, D. G., Borucki, W. J., Basri, G. et al. 2010, *ApJ*, 713, L79
- Kovari, Z., & Bartus, J. 1997, *A&A*, 323, 801
- Kretzschmar, M. 2011, *A&A*, 530, A84
- Lanza, A. F., Rodono, M., Pagano, I., Barge, P., & Llebaria, A. 2003, *A&A*, 403, 1135
- Lockwood, G. W., Skiff, B. A., Henry, G. W., Henry, S., Radick, R. R., Baliunas, S. L.,  
Donahue, R. A., & Soon, W. 2007, *ApJS*, 171, 260
- Maehara, H., Shibayama, T., Notsu, S., Notsu, Y. et al. 2012, *Nature*, 485, 478
- Notsu, S., Honda, S., Notsu, Y., et al. 2013a, *PASJ* submitted
- Noyes, R. W., Hartmann, L. W., Baliunas, S. L. et al. 1984, *ApJ*, 279, 763
- Pallavicini, R., Golub, L., Rosner, R. et al. 1981, *ApJ*, 248, 279
- Press, W. H. 1978, *Comments on Astrophysics*, 7, 103
- Randich, S. 2000, in *ASP Conf. Ser. 198, Stellar Clusters and Associations: Convection, Rotation, and Dynamos*, ed. Pallavicini, R., Micela, G. & Sciortino, S., 401
- Roettenbacher, R. M., Monnier, J. D., Harmon, R. O., et al. 2013, *ApJ*, 767, 60
- Sammis, I., Tang, F., & Zirin, H. 2000, *ApJ*, 540, 583
- Schaefer, B. E. 1989, *ApJ*, 337, 927
- Schaefer, B. E., King, J. R., & Deliyannis, C. P. 2000, *ApJ*, 529, 1026
- Segura, A., Walkowicz, L., Meadows, V., et al. 2010, *Astrobiology*, 10, 751

- Shibata, K., & Yokoyama, T. 1999, ApJ, 526, L49
- Shibata, K., & Yokoyama, T. 2002, ApJ, 577, 422
- Shibata, K., & Magara, T. 2011 Living rev. Solar Phys., 8, 6
- Shibata, K., Isobe, H., Hillier, A., et al. 2013, PASJ 65, 49, arXiv:1212.1361v1
- Shibayama, T., Maehara, H., Notsu, S., Notsu, Y., et al. 2013 ApJ submitted
- Sing, D. K., 2010, A&A, 510, A21
- Snodgrass, H. B., & Ulrich, R. K., 1990, AJ, 351, 309-316
- Solanki, S., K., 2003, A&A Rev., 11, 153
- Stumpe, M.C., Smith, J.C., Van Cleve, J.E., et al. 2012, PASP, 124, 985
- Vaughan, S. 2005, A&A, 431, 391
- Walkowicz, L. M., Basri, G., Batalha, N., et al. 2011 AJ, 141, 50
- Walkowicz, L. M., Basri, G., & Valenti, J. A. 2013, ApJS, 205, 17

Table 1: Length of the observation period during each quarter and the number of solar-type stars.

Quarter	N <sup>a</sup>	$\tau$ [days] <sup>b</sup>	Release <sup>c</sup>
0	9511	11	14 <sup>d</sup>
1	75598	33	14 <sup>d</sup>
2	82811	90	14 <sup>d</sup>
3	82586	90	14 <sup>d</sup>
4	89188	90	14 <sup>d</sup>
5	86248	95	16 <sup>e</sup>
6	82052	90	16 <sup>e</sup>

---

<sup>a</sup> Number of solar-type stars.

<sup>b</sup> Length of the observation period during each quarter.

<sup>c</sup> Release number of the data we use in this paper.

<sup>d</sup> Kepler Data Release numbers 14 Notes (Christiansen & Barclay 2012a)

<sup>e</sup> Kepler Data Release numbers 16 Notes (Christiansen & Barclay 2012b)

Table 2: Stellar parameters for three solar-type superflare-generating stars of which we show the results of model analysis in Figure 3, 4 & 5.

Kepler ID	$T_{\text{eff}}^{\text{a}}$	$\log g^{\text{a}}$	$R/R_{\odot}^{\text{a}}$	Period <sup>b</sup>	Amplitude <sup>c</sup>
6034120	5407	4.7	0.77	5.6	$4.45 \times 10^{-3}$
6691930	5348	4.5	0.95	13.1	$1.29 \times 10^{-2}$
10528043	5143	4.5	0.88	12.9	$6.52 \times 10^{-3}$

<sup>a</sup>These data are taken from the Kepler Input Catalog (Brown et al. 2011).

<sup>b</sup>The period of the largest amplitude component of the brightness variations in unit of day.

<sup>c</sup>The normalized amplitude of the dominant period.

Table 3: Best set of model parameters for Figure 3, 4 & 5.

Kepler ID	Inclination	spot name	$R_{\text{spot}}/R_{\text{phot}}$	Initial Latitude	Initial Longitude Difference
6034120	45°	spot1	0.13	41°N	–
6691930	32°	spot1	0.23	30°N	–
–	–	spot2	0.21	60°N	70°
10528043	60°	spot1	0.15	0°N	–
–	–	spot2	0.10	37°N	120°



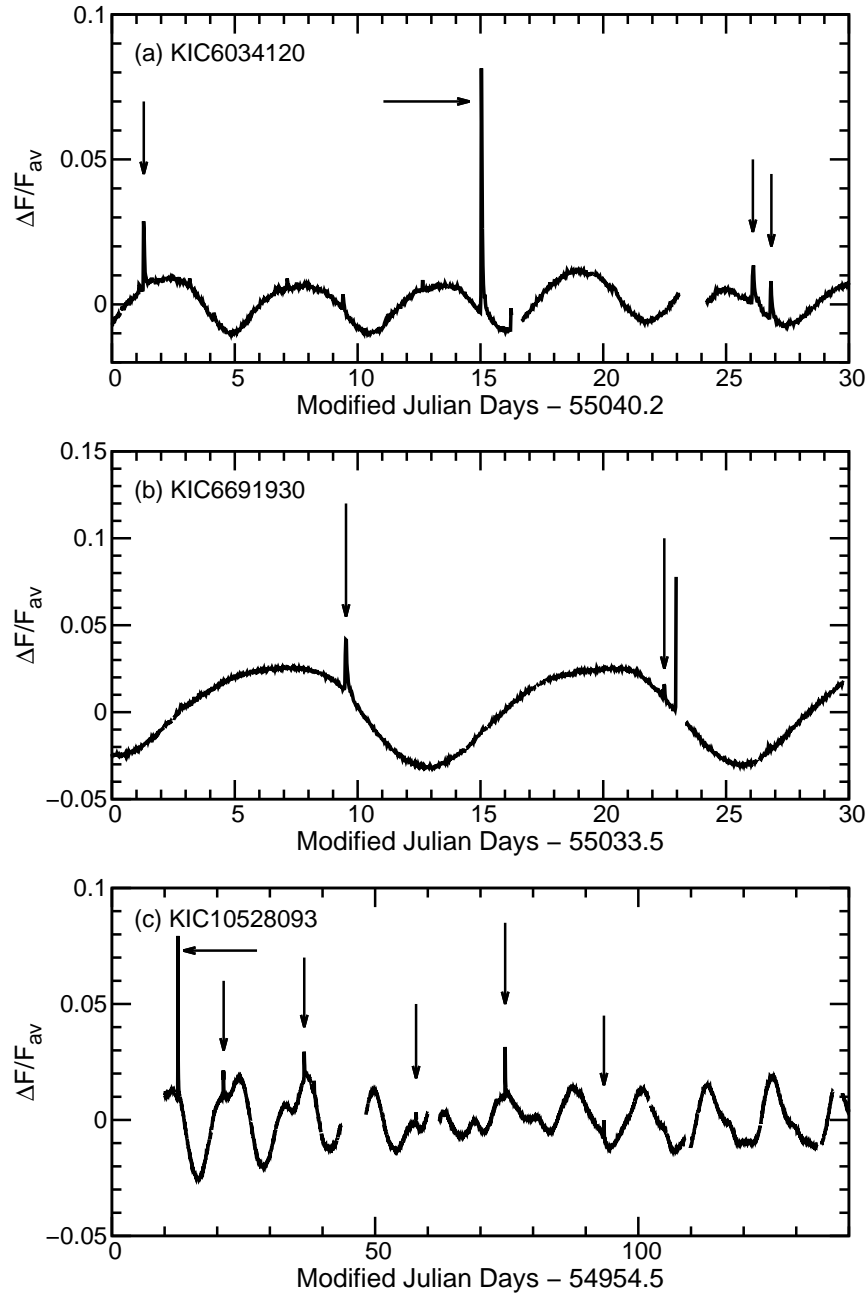


Fig. 1.— Light curve of typical superflares on solar-type stars (KIC6034120 & KIC6691930, Quarter 2; KIC10528093, Quarter 0-2). The vertical axis is the brightness variations relative to the average brightness. The typical photometric error is about 0.02 %. Arrows indicate superflares reported in Maehara et al. (2012).

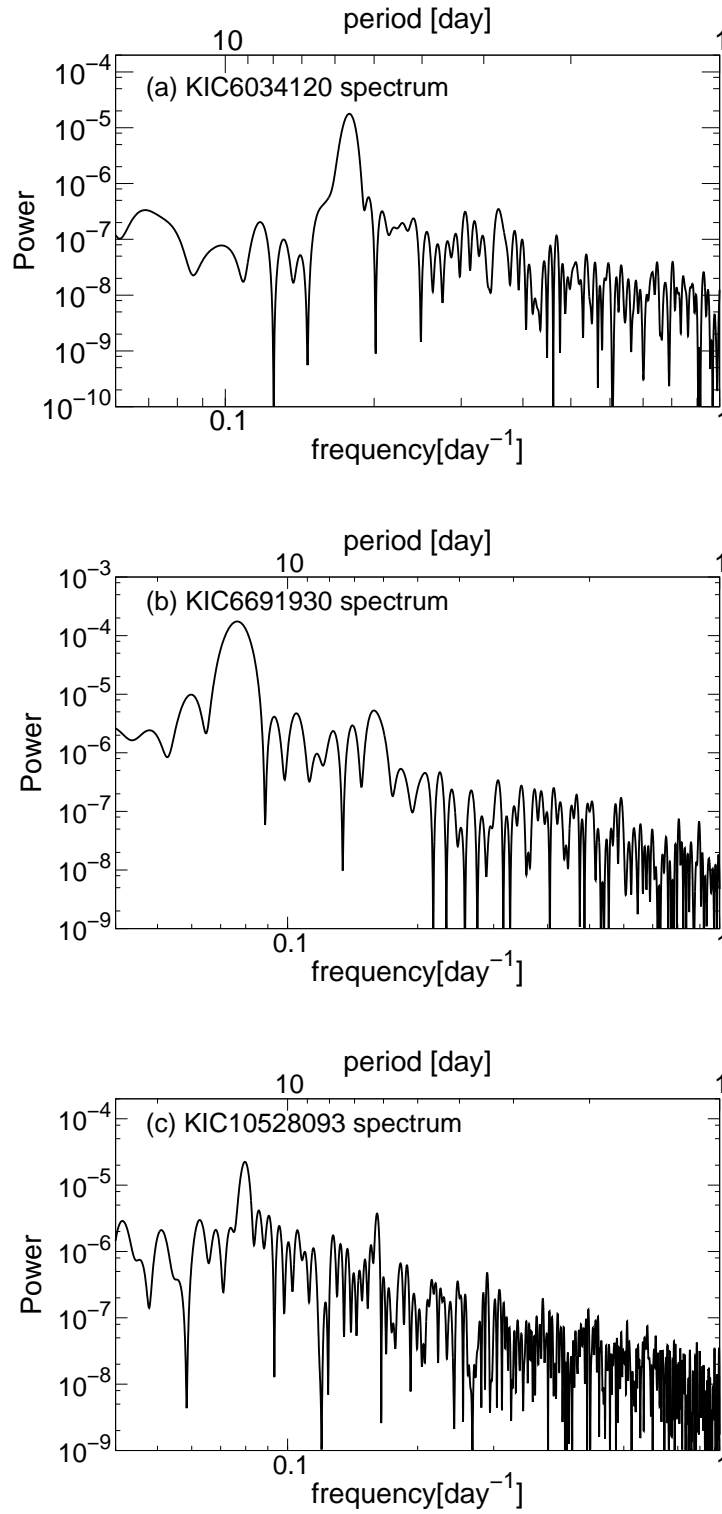


Fig. 2.— Power spectra of the light curves shown in Figure 1. The periods of these three stars are shown in Table 2.

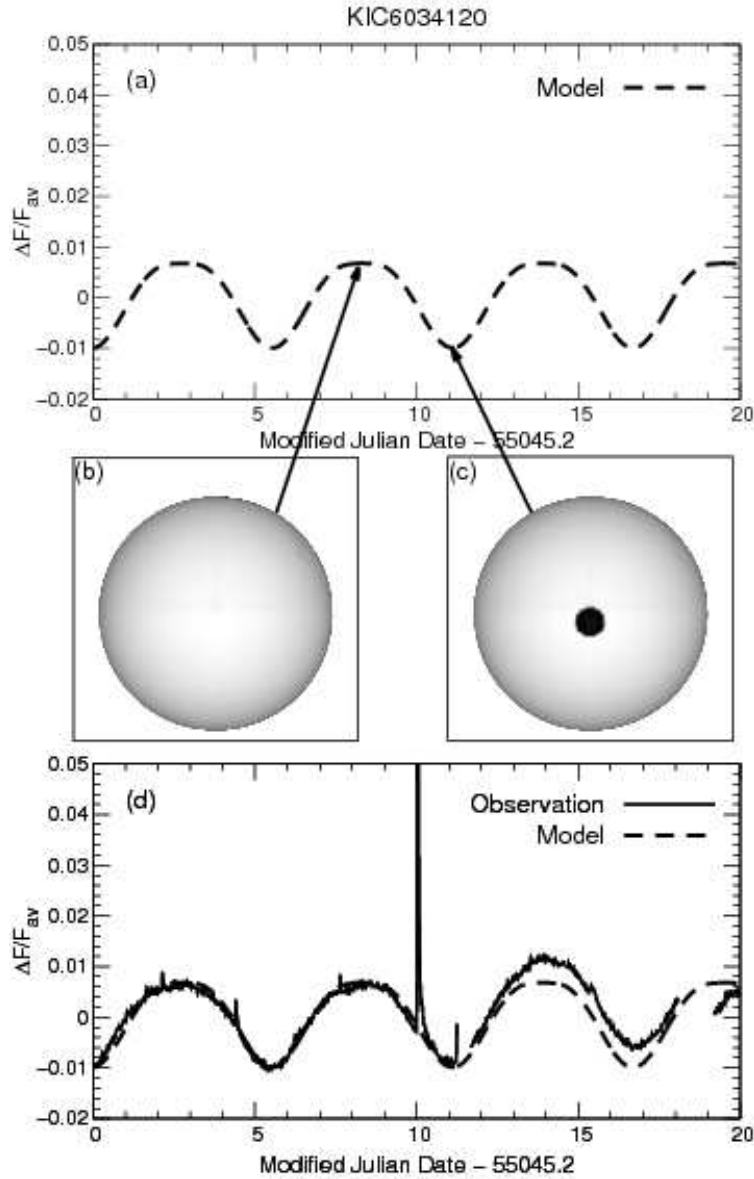


Fig. 3.— (a): Model light curve for KIC6034120 (Figure 1 (a)). The model parameters are given in Table 3. (b) & (c): Model pictures of the visible area of the photosphere with a starspot. (d): Observed light curve (solid line; the same as in Figure 1 (a)) and the model one (dashed line) for KIC6034120.

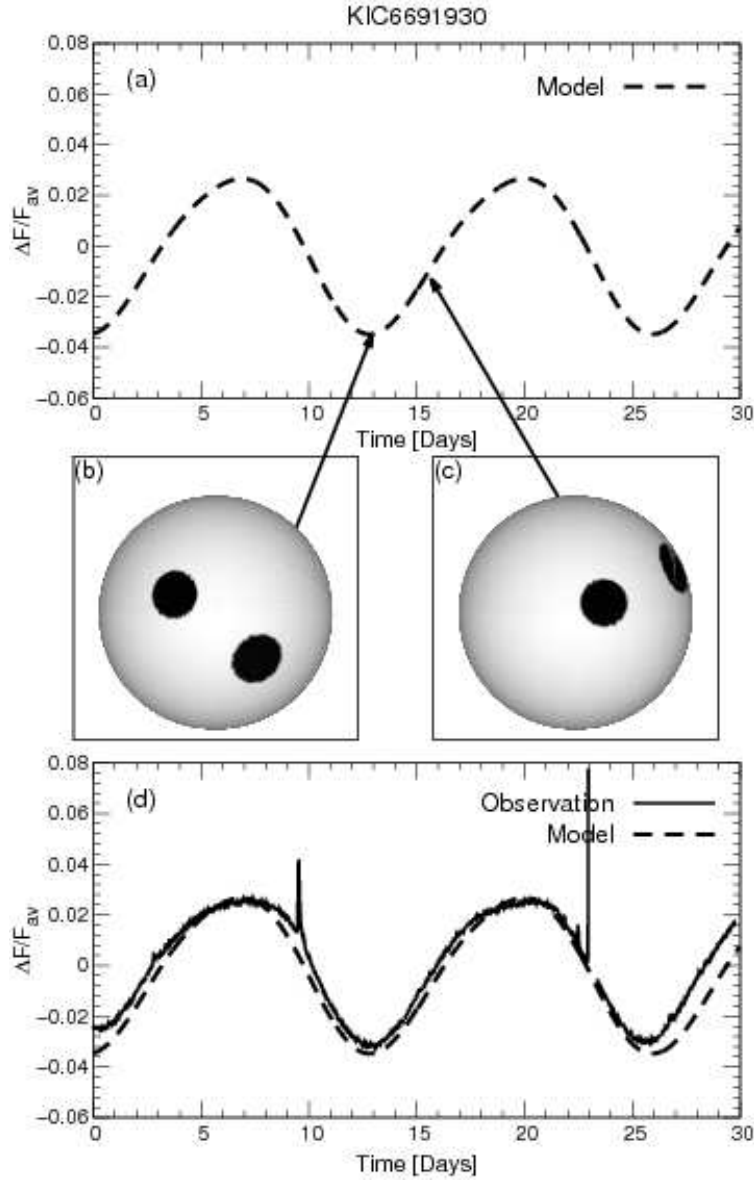


Fig. 4.— (a) : Model light curve for KIC6691930. The model parameters are given in Table 3. (b) & (c): Model pictures of the visible area of the photosphere with two starspots. (d): Observed light (solid line; the same as in Figure 1 (b)) and the model one (dashed line) for KIC6691930.

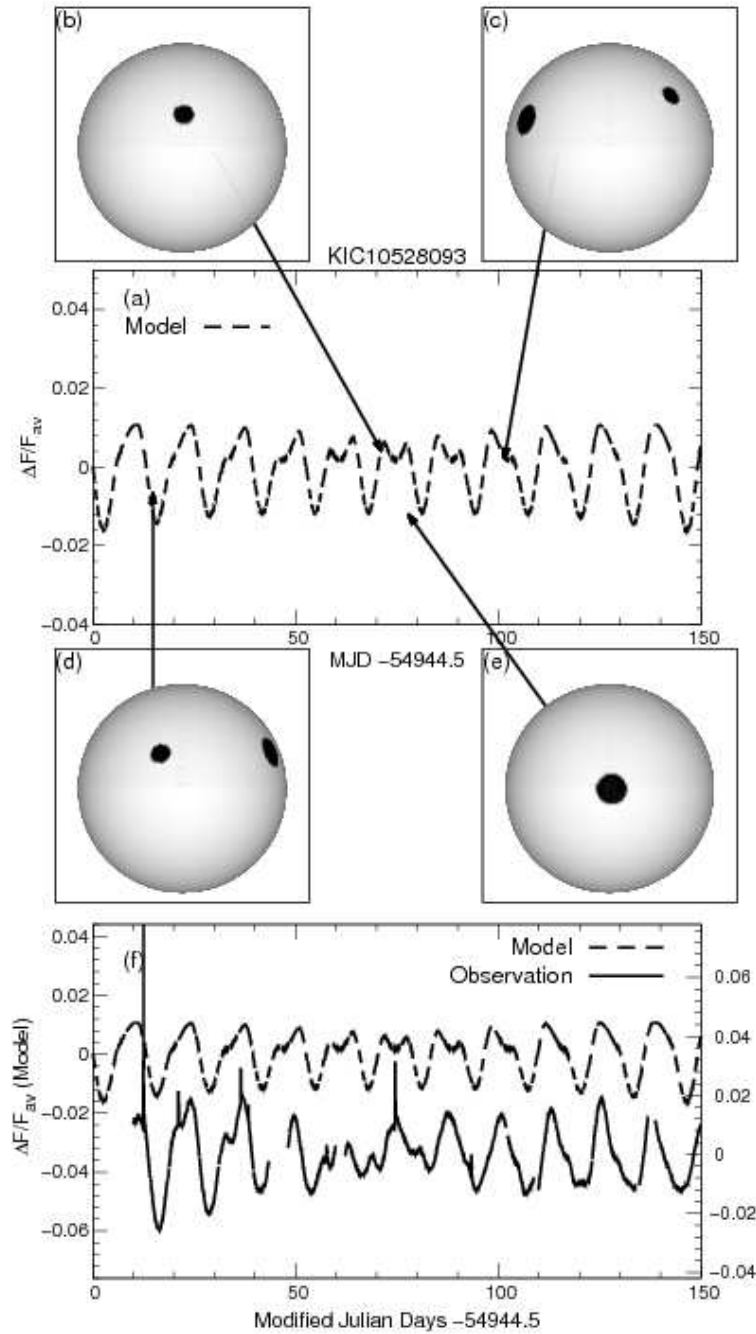


Fig. 5.— (a) Model light curve for KIC10528093. The model parameters are given in Table 3. (b), (c), (d) & (e): Model pictures of the visible area of the photosphere with starspots. (f): Observed light curve (solid line; the same as in Figure 1 (c)) and the model one (dashed line) for KIC10528093.

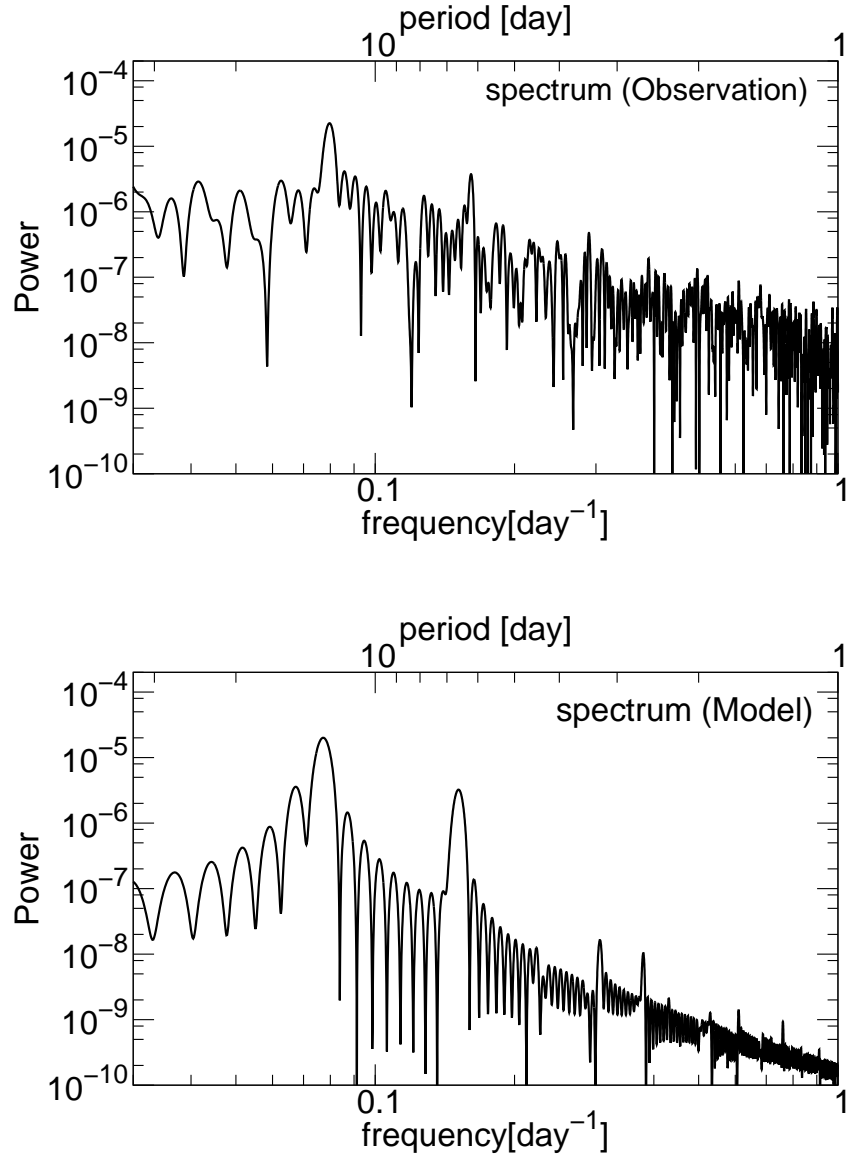


Fig. 6.— Power spectra of the period analysis for the observed light curve and for the model one of KIC10528093 shown in Figure 5(f).

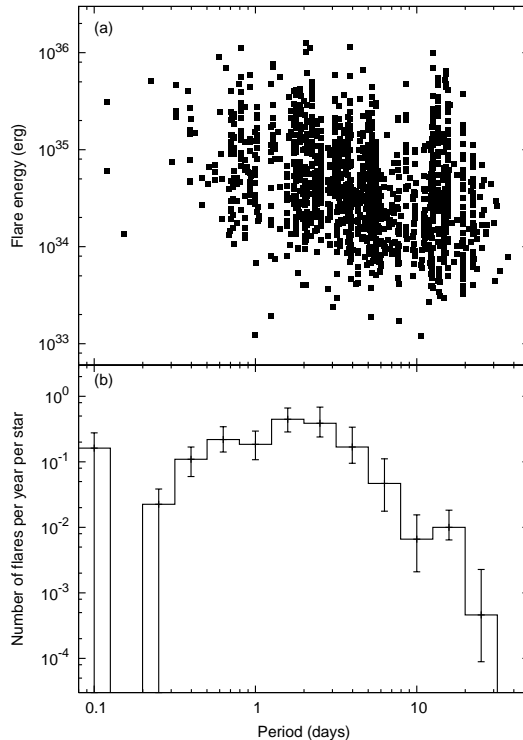


Fig. 7.— (a) Scatter plot of the flare-energy vs the brightness variation period. The period of the brightness variation in this figure was estimated by using the Kepler data of Quarter 1-6. We do not use Quarter 0 data here since the data period is shorter ( $\sim 11$  days) than other Quarters and sometimes long term variations ( $\sim 30$  days) are removed. An apparent negative correlation between the variation period and the lower limit of the flare energy results from the detection limit of our flare-search method. (b) Distribution of the occurrence of flares in each period bin as a function of the brightness variation period. The vertical axis indicates the number of flares with energy  $\geq 5 \times 10^{34}$  erg per star per year. The error bars represent the  $1\sigma$  uncertainty estimated from the square root of the event number of flares in each bin. The frequency distribution of superflares saturates for periods shorter than a few days. A similar saturation is observed for the relations between the coronal X-ray activity and the rotation period (Randich 2000). Note that these figures are a bit different from those of Figure 3 of Maehara et al. (2012); the number of flares per year per stars for stars with period between 20 and 30 days is about 30 times smaller than that of Maehara et al. (2012). Main reason of this difference is that the number of solar-type stars in longer period bins is larger than that in Maehara et al. (2012). This is because the light curves produced by the improved pipeline (PDC-MAP; e.g., Stumpe et al. (2012)) were used for the period analysis and the long-period brightness variations can be more easily detected in the improved light curves. The number of superflare stars did not change so much because these stars tend to have large starspots and it was easy to detect the long term brightness variations even in Maehara et al. (2012), which did not use PDC-MAP pipeline. (See Shibayama et al. (2013) for more details.)

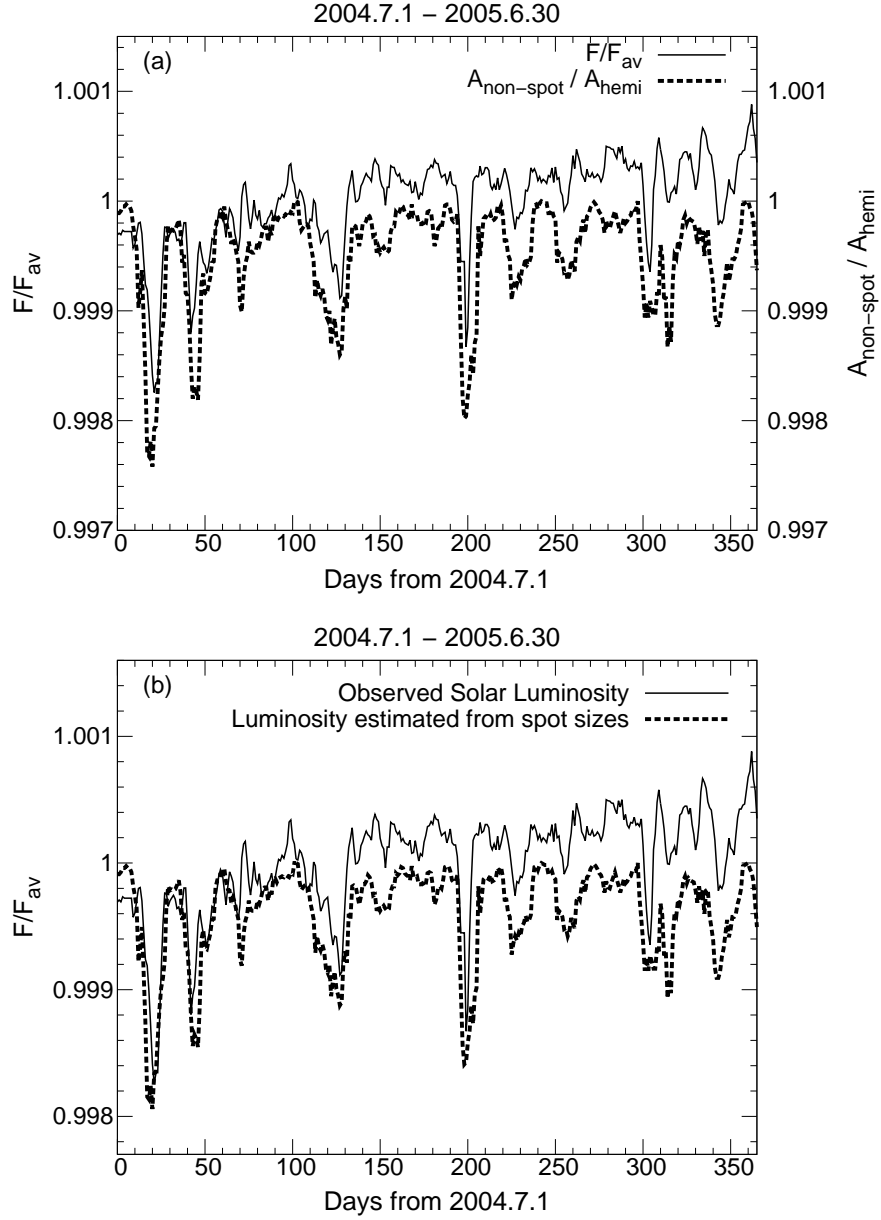


Fig. 8.— (a): Normalized irradiance of the Sun and area not covered by sunspots. The data period is 2004.7.1 - 2005.6.30. Solid lines are normalized visible (4,500-8,000Å) solar irradiance from the solar spectral irradiance data of the SORCE Satellite. We use the daily sunspots area data prepared by the U.S. Dept. of Commerce, NOAA, Space Weather Prediction Center. (b): Normalized irradiance of the Sun and the luminosity estimated from the spot coverages assuming that the temperature of sunspots is 4,000K and that of the solar photosphere is 6,000K. The data period is the same as (a).



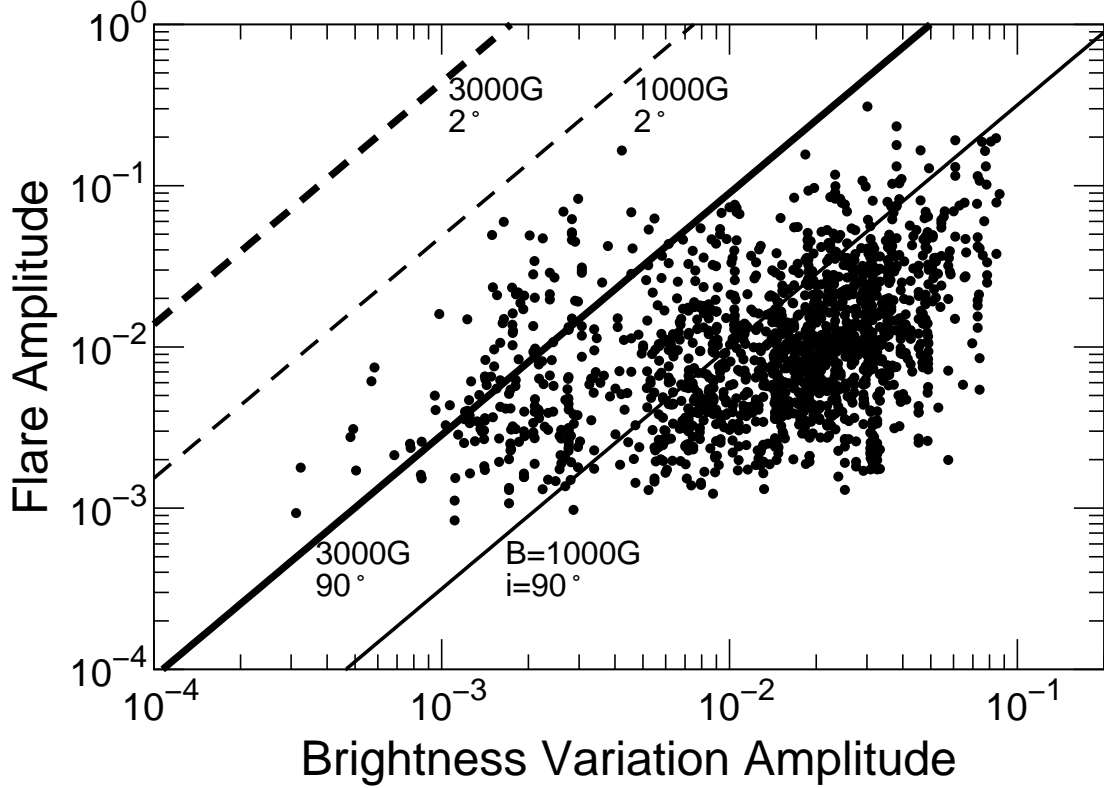


Fig. 9.— Scatter plot of superflare amplitude as a function of the amplitude of the brightness variation. The data of superflares are taken from quarter 1-6 data and are reported in Shibayama et al. (2013). We here defined the amplitude as the normalized brightness range, in which the lower 99 percent of the distribution of brightness difference from the average, except for the flares, are included. Thick and thin solid lines correspond to the analytic relation between the stellar brightness variation amplitude (corresponding to the spot area) and flare amplitude (correspond to the flare energy) obtained from equation (13) for  $B=3,000\text{G}$  and  $1,000\text{G}$ . The thick and thin dashed lines correspond to the same relation in case of nearly pole-on ( $i=2.0$  deg) for  $B=3,000\text{G}$  and  $1,000\text{G}$ . These lines are considered to give an upper limit for the flare amplitude.

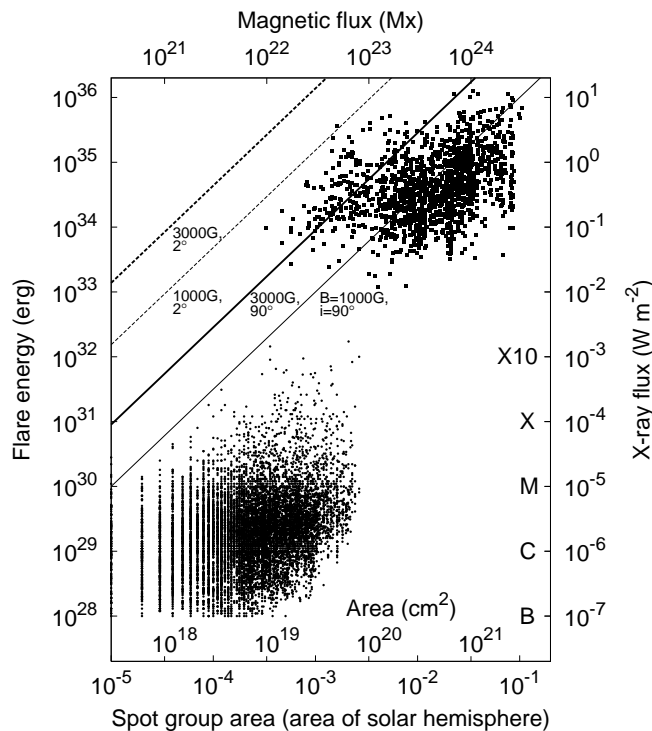


Fig. 10.— Flare energy vs spot coverage of superflares on solar-type stars (filled squares; Shibayama et al. 2013) and solar flares (filled circles; Sammis et al. 2000, Ishii 2012). The data of solar flares are taken from <ftp://ftp.ngdc.noaa.gov/STP>, and consists of data in 1989-1997 (Sammis et al. 2000) and those in 1996-2006 (Ishii 2012). Thick and thin solid lines corresponds to the analytic relation between the flare energy obtained from equation (14) for  $B=3,000\text{G}$  and  $1,000\text{G}$ . The thick and thin dashed lines correspond to the same relation in case of nearly pole-on ( $i=2.0$  deg) for  $B=3,000\text{G}$  and  $1,000\text{G}$ . These lines are considered to give an upper limit for the flare energy (i.e., possible maximum magnetic energy which can be stored near sunspots). Note that the superflare on solar-type stars is observed only with visible light and the total energy is estimated from such visible light data. Hence the X-ray intensity in the right hand vertical axis is not based on actual observations. The energy of solar flares is based on the assumption that the energy of X10-class flare is  $10^{32}$  erg, X-class  $10^{31}$  erg, M-class  $10^{30}$  erg, and C-class  $10^{29}$  erg, considering previous observational estimate of energies of typical solar flares (e.g., Benz 2010). The values on the horizontal axis at the top show the total magnetic flux of spot corresponding to the area on the horizontal axis at the bottom when  $B=1,000\text{G}$ .